Supplementary Information

Gyroid structured aqua-sheet with sub-nanometer thickness enabling 3D fast proton relay conduction

Tsubasa Kobayashi, Ya-xin Li, Ayaka Ono, Xiang-bing Zeng, Takahiro Ichikawa*

Contents

1. Synthesis of Diene-GZI

Scheme S1. Synthetic scheme for **Diene-GZI**.

Synthesis of Head group of the gemini-type amphiphiles

S1 → **S2** → **Head**
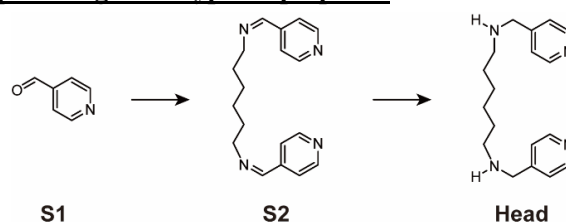
1,6-Hexanediamine (2.70 g, 23.3 mmol) was added to a solution of 4-pyridinecarboxaldehyde (**S1**) (5.00 g, 46.7 mmol) in ethanol and then heated to reflux for 4 h. The reacted solution was cooled to room temperature. NaBH$_4$ (2.16 g, 57.7 mmol) in ethanol (50ml) was gradually added to this solution and then the mixture was heated to reflux for 4 h. Excess amount of NaOH aq. and CHCl$_3$ was added to the reaction solution and the organic layer was collected and evaporated. The obtained reactant was washed with diethyl ether repeatedly and collected by filtration. White powder was obtained in 83 %. The ^{1}H NMR data were in accordance with the literature: Saeed, H. K., *et al., Angew. Chem. Int. Ed.* **56,** 12628 (2017).

Synthesis of polymerizable alkyl chain (Diene)

S3 → **S4** → **S5** → **Diene**
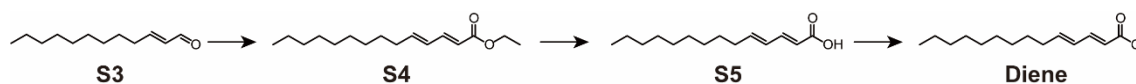
Triethyl phosphonoacetate (4.64 g, 20.7 mmol) was slowly added to a suspension of 60 % NaH (0.802 g, 20.1 mmol) and dry THF (100 ml) over 20 minutes. The mixture was stirred at room temperature until the solution became clear. Then a solution of *trans*-2-dodecene-1-al (**S3**) (4.05 g, 22.2 mmol) in dry THF (50 ml) was added dropwise. The mixture was heated to 65 °C for 30 minutes and then cooled to room temperature. Saturated NaCl aq. was added to the reaction solution and organic fraction was extracted by ethyl acetate. The evaporation gave a yellow liquid (**S4**).

Methanol (100ml) solution, water (5 ml) and NaOH (0.90 g, 22.5 mmol) were added to the **S4** and the mixture was heated to 60 °C for 3 h. The reaction solution was evaporated and washed with hexane/acetone (50/50, v/v) repeatedly and then white powder was obtained by filtration. The filtrated powder was added to an excess amount of HCl aq. and vigorously stirred for 2 h and then extracted by CHCl$_3$. The organic fraction was evaporated to give a yellowish white powder (**S5**) (yield: 77 %). The ^{1}H NMR data were in accordance with the literature: Matsumoto, A., *et al.*, *Polym. J.* **35,** 652 (2003).

The obtained carbonic acid was converted into the corresponding acid chloride by stirring in a solution of CH$_2$Cl$_2$, DMF (3 drops) and thionyl chloride at room temperature for 2 h. The resulting mixture was used without further purification.

Synthesis of Diene-GZI
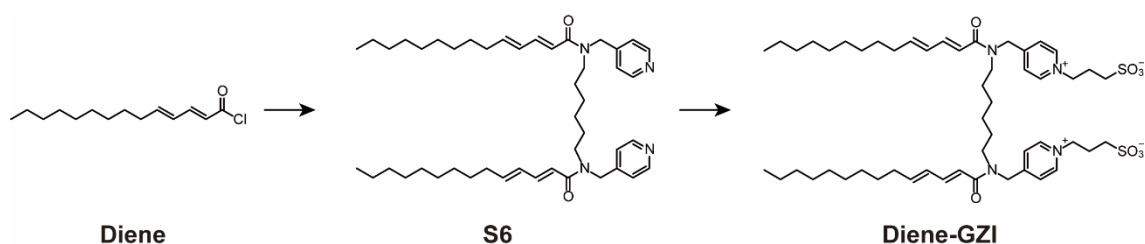
Diene (1.76 g, 8.38 mmol) was added to a solution of **Head** (1.00 g, 3.35 mmol), triethylamine (1.69 g, 16.8 mmol) and a small amount of 4-dimethylaminopyridine in CH_2Cl_2 (100 ml) at 0 °C for 1 h. Then water and $CHCl_3$ were added. The organic layer was separated and evaporated. The crude product was purified by flash column chromatography (silica gel, eluent: $CHCl_3$/methanol = 9/1). **S6** was obtained as a brownish oil with 76% yield.

^{1}H NMR (400 MHz, $CDCl_3$): δ = 8.56 (m, 4H), 7.39-7.35 (m, 4H), 7.13 (m, 4H), 6.25-6.02 (m, 6H), 4.61 (d, 4H), 3.48-3.27 (m, 4H), 2.18-2.12 (m, 4H), 1.56-1.27 (m, 36H), 0.87 (t, J = 6.8 Hz, 6H) . ^{13}C NMR (100MHz, $CDCl_3$: solvent peak of $CDCl_3$: δ = 77.16): δ = 167.25, 149.91, 147.23, 144.65, 128.55, 122.63, 121.42, 117.10, 58.32, 33.12, 31.94, 29.60, 29.52, 29.37, 29.28, 28.85, 28.77, 27.63, 26.70, 22.74, 14.20.

An excess amount of 1,3-propanesultone was added to a solution of crude compound of **S6** (1.80 g, 2.50 mmol) in toluene/acetonitrile/2-propanol (10/10/1, v/v/v). The mixture was heated to reflux for 8 h. Through recrystallization from $CHCl_3$/acetone mixed solvent repeatedly, **Diene-GZI** was obtained as a yellowish powder with 79% yield.

^{1}H NMR (400MHz, CD_3OD+$CDCl_3$: solvent peak of CH_3OH: δ = 3.34, $CHCl_3$: δ = 7.60): δ = 9.03-8.94 (m, 4H), 7.88 (d, J = 3.2 Hz, 4H), 7.31 (m, 2H), 6.39-5.98 (m, 6H), 4.87 (s, 4H), 4.87-4.81 (m, 4H), 3.56-3.53 (m, 4H), 2.87-2.83 (t, J = 6.8 Hz, 4H), 2.48-2.42 (m, 4H), 2.24-2.19 (m, 4H), 1.70 (m, 4H), 1.46-1.42 (m, 8H) 1.28 (m, 24H), 0.89 (m, J = 6.8 Hz, 6H)

^{13}C NMR (100MHz, CD_3OD+$CDCl_3$: solvent peak of CD_3OD: δ = 48.66, $CDCl_3$: δ =77.58): δ = 168.20, 159.42, 145.55, 144.97, 144.52, 128.52, 126.30, 125.86, 116.38, 59.39, 46.75, 33.01, 31.84, 29.60, 29.47, 29.39, 29.24, 29.16, 28.69, 27.12, 26.46, 26.25, 22.59, 13.77.

Elemental analysis. Calcd for $C_{52}H_{82}N_4O_8S_2$ 1.8H_2O: C, 63.23; H, 8.74; N, 5.67. Found: C, 63.62; H, 9.05; N, 5.65.
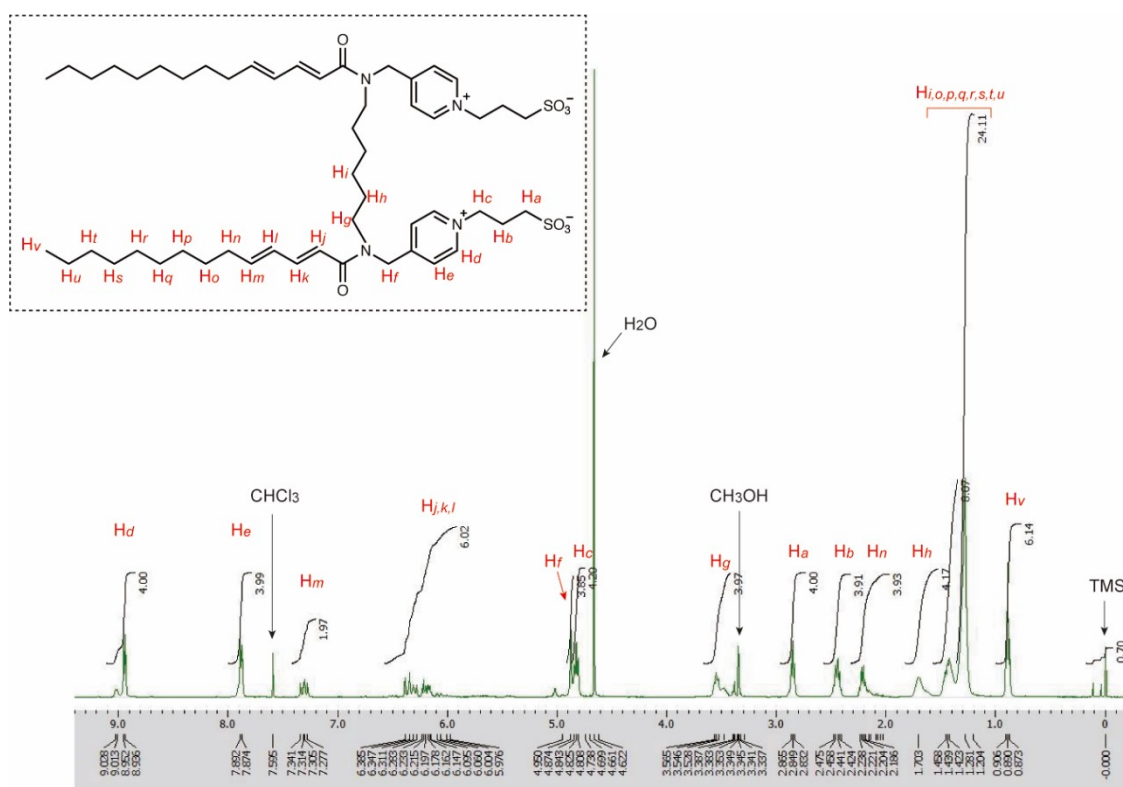
Figure S1. ^{1}H NMR spectrum of **Diene-GZI**.
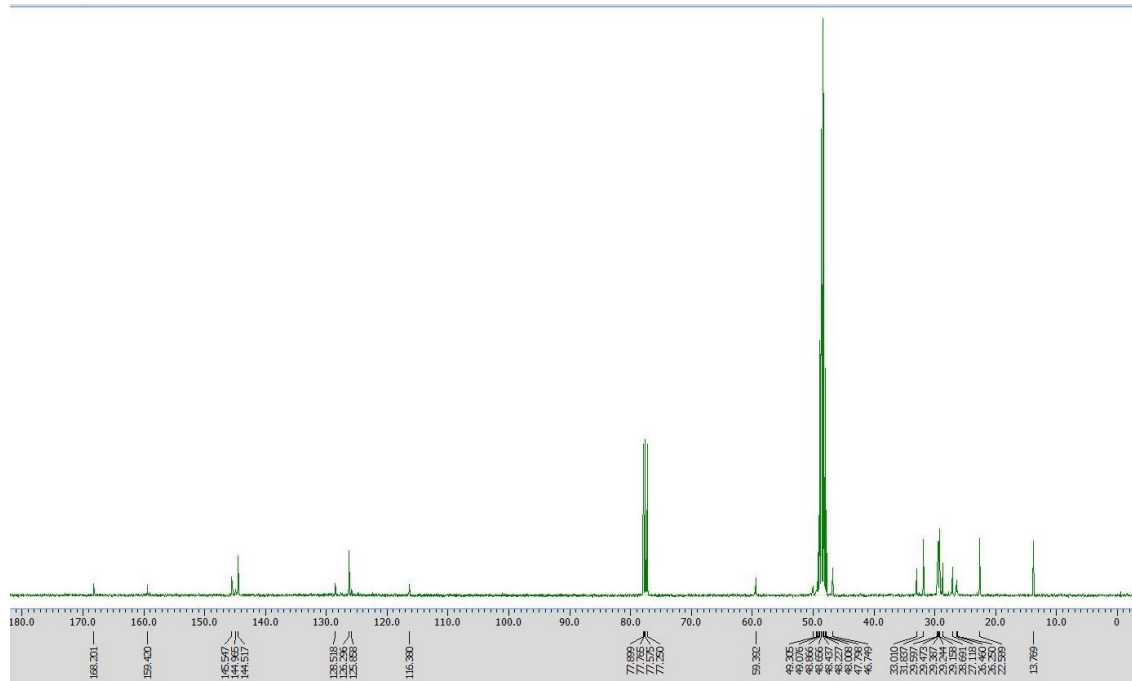
Figure S2. ^{13}C NMR spectrum of **Diene- GZI**.

2. Thermal behavior of Diene-GZI
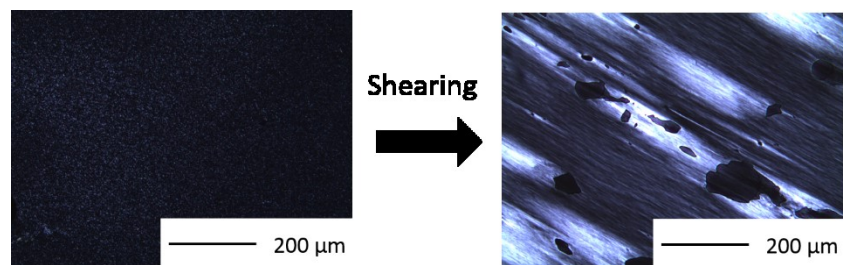
Figure S3. Polarizing optical microphotographs of **Diene-GZI** in the LC state at 100 °C before and after shearing.
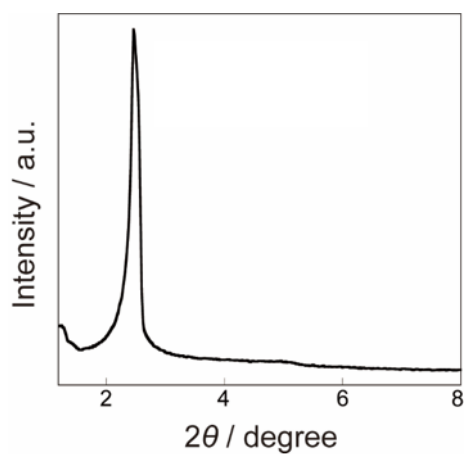
Figure S4. Wide-angle X-ray diffraction pattern of **Diene-GZI** in the LC state at 25 °C.
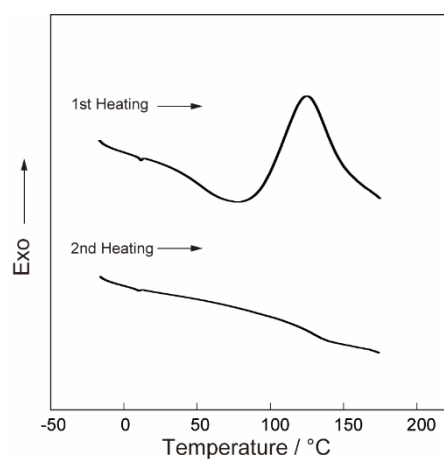
Figure S5. Differential scanning calorimetry thermograms of **Diene-GZI**.

3. Thermal behavior of MX
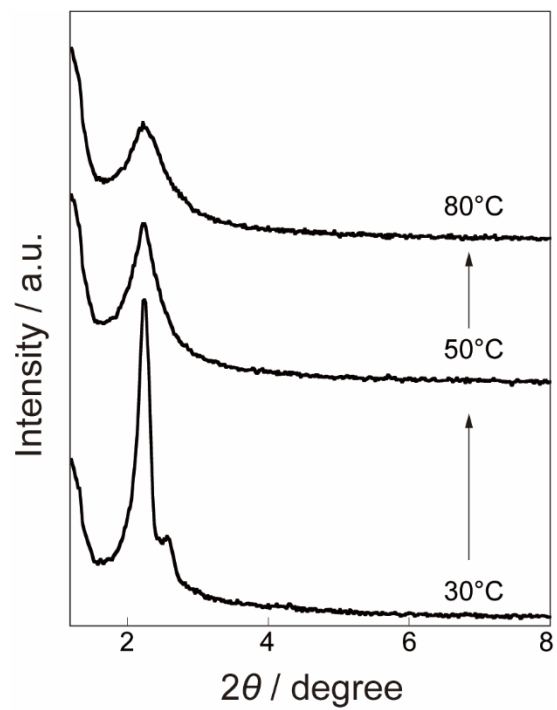
Figure S6. Wide-angle X-ray diffraction patterns of **MX** at various temperatures.

4. A molecular structure of N-MZI and its liquid-crystalline behavior
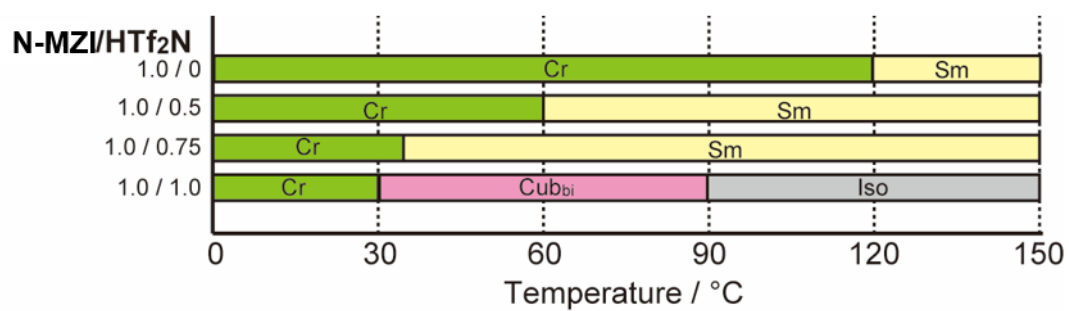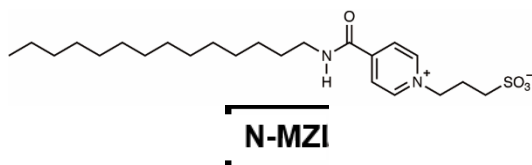
Figure S7. Thermotropic liquid-crystalline behavior of the mixtures of the **N-MZI** and HTf$_2$N in various molar rations.

Cr; crystalline, Sm; smectic, Cub$_{bi}$; bicontinuous cubic, Iso; isotropic liquid.

5. Microscopic structure in Film-Cub$_{bi}$
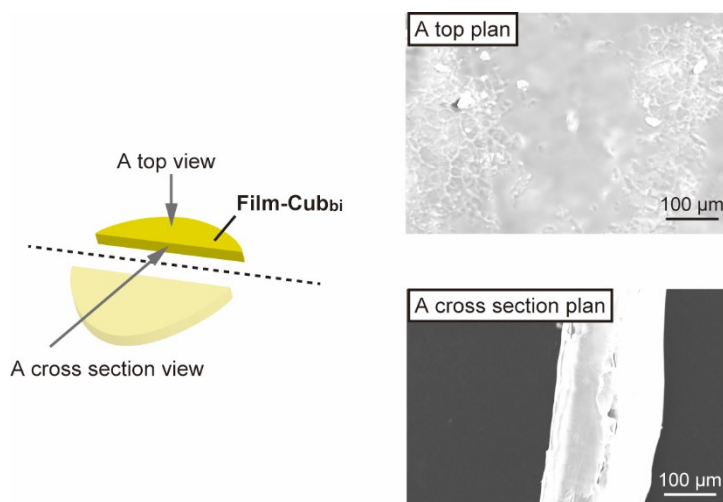
Figure S8. Macroscopic structure in **Film-Cub$_{bi}$** and its surface. Scanning electron microscope (SEM) images of **Film-Cub$_{bi}$**. A floor and cross section plans are shown.

6. IR spectra of Film-Cub$_{bi}$
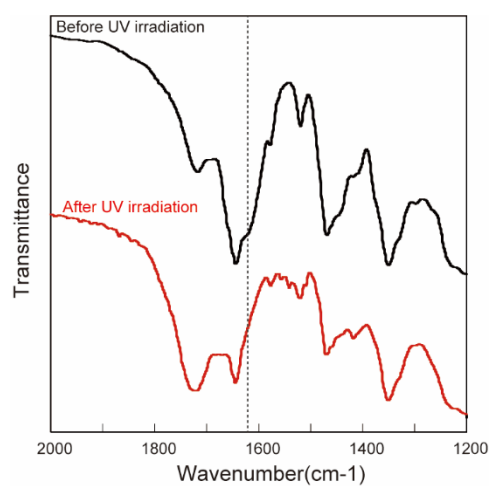
Figure S9. IR spectra of **MX** (before UV irradiation) and **Film-Cub$_{bi}$** (after UV irradiation).

7. Relative humidity dependence of the cubic lattice length in Film-Cub$_{bi}$
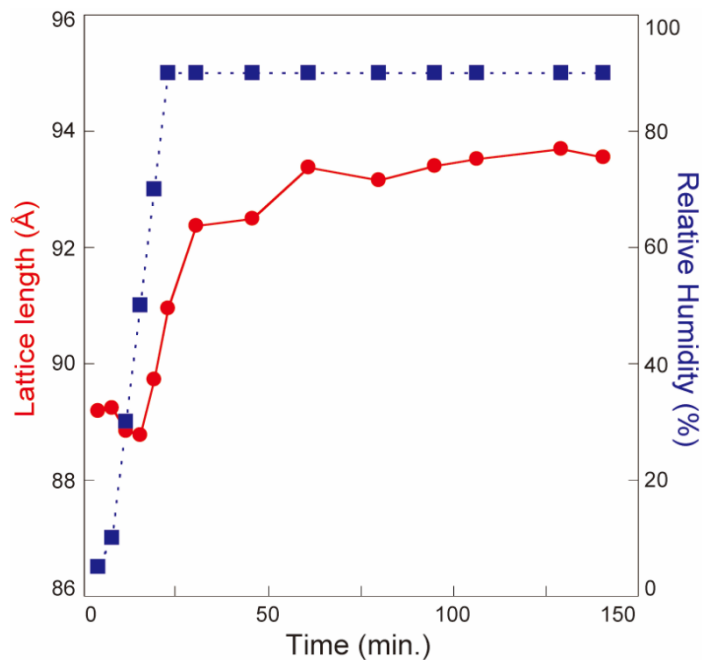
Figure S10. XRD measurements were performed for **Film-Cub$_{bi}$** with varying relative humidity (RH) at 30 °C. RH was controlled by RIGAKU Corporation. Increase speed of the cubic lattice length gradually becomes slow at around 50 minutes, suggesting that **Film-Cub$_{bi}$** reaches an equilibrium state where water absorption and evaporation into/from **Film-Cub$_{bi}$** occur in the same speed.

8. Gravimetric analysis for Film-Cub$_{bi}$ under humidity-controlled condition

Table S1. Weights of **Film-Cub$_{bi}$** before and after polymerization are shown. In addition, the weights of **Film-Cub$_{bi}$** after being placed under various RH conditions (RH = 50, 60, 70, 80, and 90) are also measured. By using these values, the water weights (mg) and water contents (wt %) in **Film-Cub$_{bi}$** were estimated.

	Weight (mg)	Δ weight (mg)	Water weight (mg)	Water content (wt%)
Before Polymerization	38.58	0.00	7.21	18.7
After Polymerization	34.11	-4.47	2.74	8.05
Film-Cubbi (RH=50%)	33.61	-4.97	2.24	6.68
Film-Cubbi (RH=60%)	34.27	-4.31	2.90	8.48
Film-Cubbi (RH=70%)	35.18	-3.40	3.81	10.84
Film-Cubbi (RH=80%)	36.09	-2.49	4.72	13.09
Film-Cubbi (RH=90%)	37.14	-1.44	5.77	15.55

9. Synchrotron X-ray diffraction pattern of Film-Cub$_{bi}$

Synchrotron X-ray diffraction experiments were carried out at station I22, Diamond Light Source. A monochromatic wavelength of 1.0 Å was used and sample to detector distance was calibrated using AgBeh. A Pilatus 2M detector was used to collect the SAXS diffractograms which is then converted to 1D curves by radial integration. The samples were held in glassy capillaries (diameter: 1.0mm), with or without water, and for dried samples sealed to avoid effect of humidity in the air.

   In the experiments, two intense peaks and six weak peaks are observed. Their reciprocal d-spacing ratio of these peak is √6:√8:√14:√16:√20:√22:√24:√26. The observed diffraction peaks can only be indexed by a body centered cubic lattice with indices (211), (220), (321), (400), (420), (332), (422) and (431). An alternative indexing to a primitive lattice is not possible. If you index the first two peaks as (111) and (200) instead, the 3rd peak should have $h^2+k^2+l^2$ equal to 7 which is impossible. The (hkl) indices conforms strictly to the $Ia3d$ space group symmetry: $h+k+l$ is always even, for ($hk0$) peaks both h and k are even, for (hhl) peaks $2h+l=4n$, and for ($h00$) peak $h=4n$. All unobserved peaks (100), (110), (111), (200), (210), (300), (310), (311), (222), (320), (410), (411), (330), (331), (421), and so on are expected to be extinct by the $Ia3d$ space group symmetry.
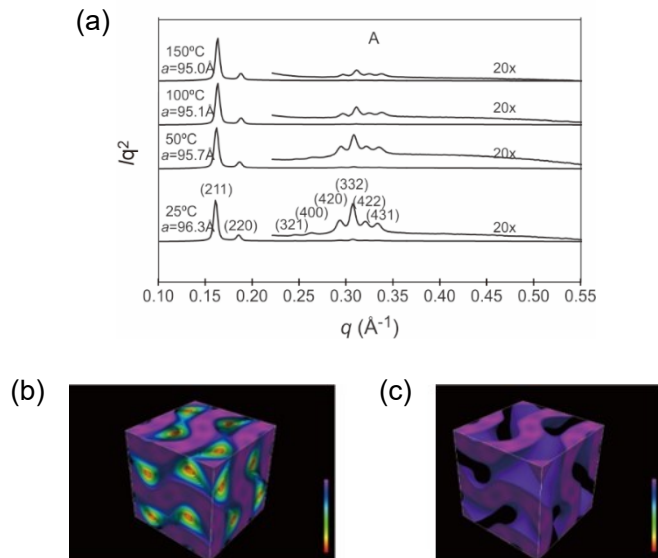
Figure S11. (a) XRD patterns of **Film-Cub$_{bi}$** measured by synchrotron X-ray diffraction measurement. (b) Reconstructed electron density map. (c) Reconstructed electron density map of highest region.

10. Material density measurement for Film-Cub$_{bi}$

Material densities of the driest **Film-Cub$_{bi}$** and the wettest **Film-Cub$_{bi}$** are determined by floating the films into mixed solvents of chloroform (d = 1.49 g cm^{-3}) and hexane (d = 0.66 g cm^{-3}) in various ratios. It has been found that the driest film starts to float when the density of the solvent reach 1.27 g cm^{-3} whereas wettest film starts to float when the density of the solvent reach 1.17 g cm^{-3}.
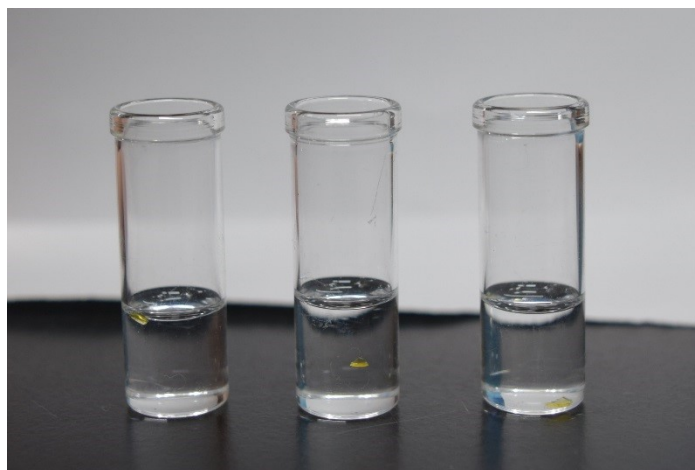
Figure S12. Driest **Film-Cub$_{bi}$** in chloroform (left), chloroform/hexane mixture (3/1 by volume) (middle), chloroform/hexane mixture (1/1 by volume) (right).

The cubic lattice length of the driest **Film-Cub$_{bi}$(1.2)** was found to be 89.6 Å (a_0) while that of the wettest **Film-Cub$_{bi}$(X$_{wettest}$)** was found to be 105.6 Å (a). The amount of the absorbed water weight in a cubic lattice is calculated from $1.17a^3 - 1.27a_0^3$ (H$_2$O$_{abs}$). The initial water content of the driest **Film-Cub$_{bi}$(1.2)** in a cubic lattice is $1.27a_0^3 \times 0.012$ (H$_2$O$_{init}$). We estimated the water content **X$_{wettest}$** from (H$_2$O$_{abs}$ + H$_2$O$_{init}$)/ $1.17a^3 \times 100$ to be 34.5 wt%.
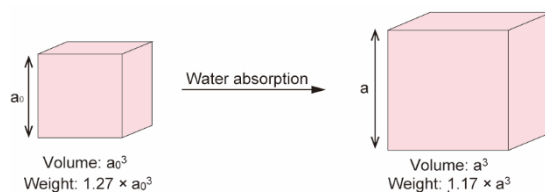
11. Preparation of samples with various water contents for synchrotron X-ray diffraction measurements

For the Synchrotron X-ray measurement for **Film-Cub$_{bi}$(X)** with various X values, we prepared various **Film-Cub$_{bi}$(X)** by putting it under various conditions, such as dried at 110 °C, dried at 80 °C, vacuum dried at room temperature, no treatment, wet, after soaked in water for 3 h, and immersed in water. Since it was impossible to perform gravimetric analysis for these films, we made an assumption below to estimate the water content X.

Assuming that the cubic lattice length in **Film-Cub$_{bi}$(X)** increase linearly against the water content X, we obtained an equation $Y = 0.4805X + 89.0$ by using these data of the driest **Film-Cub$_{bi}$** and the wettest **Film-Cub$_{bi}$**.

$y = 0.4805x + 89.023$
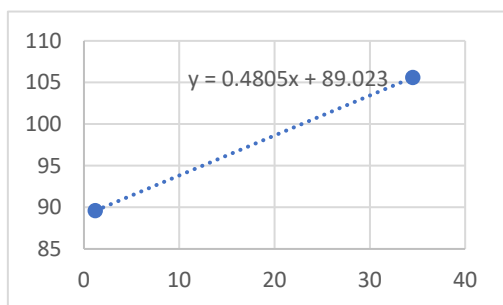
Table S2. Water contents calculated from the lattice parameter.

Lattice parameter Y (Å)	Water content (wt%) from experiment	Water content (wt%) from calculation
89.7	1.2	1.2
91.6	-	5.4
93.5	-	9.3
94.5	-	11.4
97.2	-	17.0
100.7	-	24.3
105.6	-	34.5

12. Reconstruction of electron density maps

The intensities and phases used to reconstruct the electron density maps are listed in the tables below.

Table S3. The indices, experimental, calculated d-spacings, intensities, phases and lattice parameter of **Film-Cub$_{bi}$ with 1.2 wt% H$_2$O** obtained from SAXS. All intensity values are Lorentz corrected.

(hk)	d-spacing (nm) experimental	d-spacing (nm) calculated	Intensity	Phase
(211)	3.66	3.66	100.00	0
(220)	3.17	3.17	13.62	0
(321)	-	2.40	-	-
(400)	-	2.24	-	-
(420)	2.01	2.01	0.19	0
(332)	1.91	1.91	0.67	π
(432)	1.83	1.83	0.34	π
(431)	1.76	1.76	0.30	π
a = 8.97 nm				

Table S4. The indices, experimental, calculated d-spacings, intensities, phases and lattice parameter of **Film-Cub$_{bi}$ with 5.4 wt% H$_2$O** obtained from SAXS. All intensity values are Lorentz corrected.

(hk)	d-spacing (nm) experimental	d-spacing (nm) calculated	Intensity	Phase
(211)	3.74	3.74	100.00	0
(220)	3.24	3.24	12.43	0
(321)	-	2.45	-	-
(400)	-	2.29	-	-
(420)	2.04	2.05	0.53	0
(332)	1.95	1.95	1.60	π
(432)	1.87	1.87	0.69	π
(431)	1.80	1.80	0.59	π
a = 9.16 nm				

Table S5. The indices, experimental, calculated *d*-spacings, intensities, phases and lattice parameter of **Film-Cub$_{bi}$ with 9.3 wt% H$_2$O** obtained from SAXS. All intensity values are Lorentz corrected.

(*hk*)	*d*-spacing (nm) experimental	*d*-spacing (nm) calculated	*Intensity*	*Phase*
(211)	3.78	3.78	100.00	0
(220)	3.27	3.27	12.22	0
(321)	-	2.47	-	-
(400)	2.32	2.32	0.07	0
(420)	2.07	2.07	0.56	0
(332)	1.97	1.97	1.66	π
(432)	1.89	1.89	0.61	π
(431)	1.82	1.82	0.54	π
a = 9.26 nm				

Table S6. The indices, experimental, calculated *d*-spacings, intensities, phases and lattice parameter of **Film-Cub$_{bi}$ with 11.4 wt% H$_2$O** obtained from SAXS. All intensity values are Lorentz corrected.

(*hk*)	*d*-spacing (nm) experimental	*d*-spacing (nm) calculated	*Intensity*	*Phase*
(211)	3.86	3.86	100.00	0
(220)	3.34	3.34	12.58	0
(321)	2.53	2.53	0.07	0
(400)	2.36	2.36	0.14	0
(420)	2.11	2.11	1.01	0
(332)	2.01	2.01	2.69	π
(432)	1.93	1.93	1.06	π
(431)	1.85	1.85	0.85	π
a = 9.45 nm				

Table S7. The indices, experimental, calculated d-spacings, intensities, phases and lattice parameter of **Film-Cub$_{bi}$ with 17.0 wt% H$_2$O** obtained from SAXS. All intensity values are Lorentz corrected.

(hk)	d-spacing (nm) experimental	d-spacing (nm) calculated	Intensity	Phase
(211)	3.97	3.97	100.00	0
(220)	3.44	3.44	12.73	0
(321)	2.60	2.60	0.48	0
(400)	2.43	2.43	0.67	0
(420)	2.17	2.17	2.98	0
(332)	2.07	2.07	7.33	π
(432)	1.98	1.98	2.52	π
(431)	1.91	1.91	1.72	π
a = 9.72 nm				

Table S8. The indices, experimental, calculated d-spacings, intensities, phases and lattice parameter of **Film-Cub$_{bi}$ with 24.3 wt% H$_2$O** obtained from SAXS. All intensity values are Lorentz corrected.

(hk)	d-spacing (nm) experimental	d-spacing (nm) calculated	Intensity	Phase
(211)	4.11	4.11	100.00	0
(220)	3.56	3.56	14.97	0
(321)	2.69	2.69	1.36	0
(400)	2.52	2.52	1.47	0
(420)	2.25	2.25	5.39	0
(332)	2.15	2.15	13.23	π
(432)	2.06	2.06	4.24	π
(431)	1.98	1.97	2.68	π
a = 10.07 nm				

Table S9. The indices, experimental, calculated *d*-spacings, intensities, phases and lattice parameter of **Film-Cub$_{bi}$ with 34.5 wt% H$_2$O** obtained from SAXS. All intensity values are Lorentz corrected.

(*hk*)	*d*-spacing (nm) experimental	*d*-spacing (nm) calculated	*Intensity*	*Phase*
(211)	4.31	4.31	100.0	0
(220)	3.73	3.73	16.91	0
(321)	2.82	2.82	2.15	0
(400)	2.64	2.64	1.12	0
(420)	2.36	2.36	11.24	0
(332)	2.25	2.25	26.91	π
(432)	2.16	2.16	14.79	π
(431)	2.07	2.07	5.84	π
a = 10.56 nm				
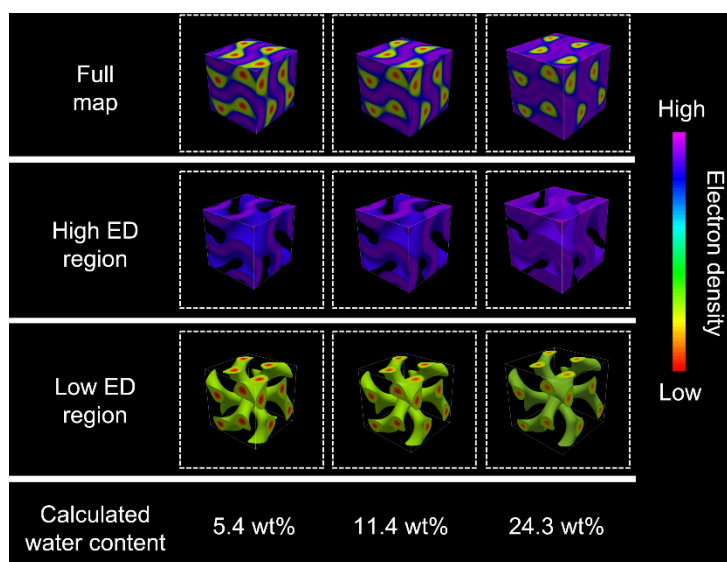
Figure S13. Reconstructed electron density maps of **Film-Cub$_{bi}$(X)** with various water contents. The highest electron density region is coloured with purple. The lowest electron density region is coloured with red.

13. Calculation of the surface area of a gyroid minimal surface

Torquato and co-workers simulated total surface area of gyroid surfaces with various mean curvature[1]. When a mean curvature equals to zero, that surface is defined as a gyroid minimal surface in a cubic lattice. Assuming the length of the cubic lattice as L, the surface area of the gyroid minimal surface is about 3.10 times as large as $L \times L$. With this, we calculated the surface area of the gyroid minimal surface in a cubic lattice in **Film-Cub$_{bi}$** with a cubic lattice length of 95 Å (A_G).

$$A_G = 95 \,(\text{Å}) \times 95 \,(\text{Å}) \times 3.10$$

Roughly assuming a water molecule as a sphere with 1.5 Å radius, the number of water molecules required for fulfilling the gyroid minimal surface is estimated as below.

$$A_G / 1.5 \,(\text{Å}) \times 1.5 \,(\text{Å}) \times \pi = 3960$$

Assuming that the density of **Film-Cub$_{bi}$** is 1.17 g/ cm^{-3}, the water content (wt %) in **Film-Cub$_{bi}$** containing 3960 water molecules can be calculated as follow.

$$100 \times (3960 \times 18 / 6.02 \times 10^{23}) / \{(9.5 \times 10^{-7})^3 \times 1.0\} = 11.8 \,(\text{wt \%})$$
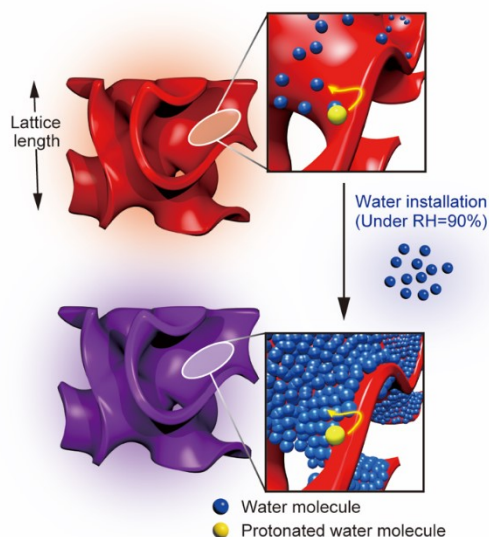
Figure S14. Schematic image of installation of water molecules on a gyroid minimal surface. Considering that **Film-Cub$_{bi}$** contains water content of 15.6 wt% at RH = 90%, it is expected that the gyroid minimal surface is fully covered with water molecules.

14. Characterization of Film-Meso
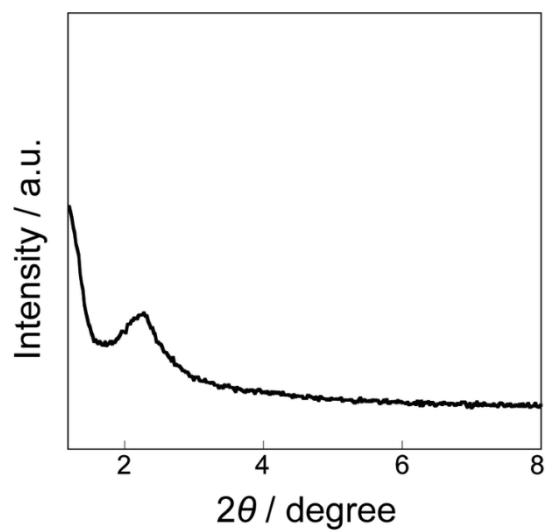
Figure S15. Wide-angle X-ray diffraction pattern of **Film-Meso** at 30 °C.

15. Synthetic scheme for GZI
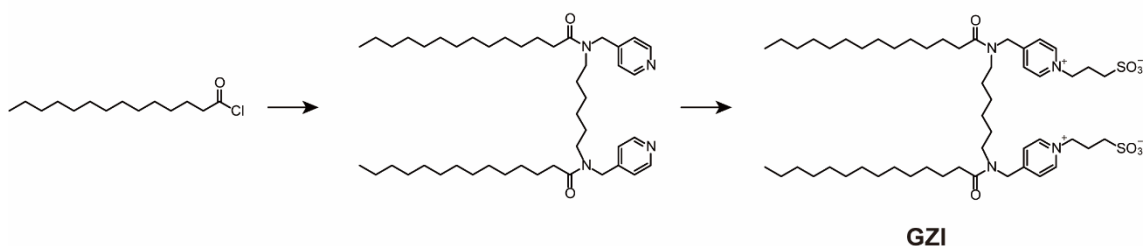
Myristoyl chloride was added dropwise to a solution of **Head** (1.00 g, 3.35 mmol), triethylamine (1.69 g, 16.8 mmol) and a small amount of 4-dimethylaminopyridine in CH_2Cl_2 (100 ml) at 0 °C and stirred for 1 h. The reaction was quenched by water, and organic components were extracted by $CHCl_3$. The organic layer was separated and evaporated. The crude product was purified by flash column chromatography (silica gel, eluent: $CHCl_3$/methanol = 9/1). This precursor of **GZI** was obtained as a yellowish oil with 75% yield.

An excess amount of 1,3-propanesultone was added to a solution of the precursor (1.80 g, 2.50 mmol) in toluene/acetonitrile/2-propanol (10/10/1, v/v/v). The mixture was heated to reflux for 8 h. Through recrystallization from $CHCl_3$/acetone mixed solvent repeatedly, **GZI** was obtained as a white powder with 75% yield.

^{1}H NMR (400 MHz, CD$_3$OD+CDCl$_3$): δ = 8.93 (d, J = 6.4 Hz 4H), 7.89 (d, J = 6.4 Hz 4H), 7.62 (solvent: CHCl$_3$), 4.87-4.82 (m, 8H), 3.47 (m, 4H), 3.34 (solvent: CH$_3$OD), 2.84 (m, 4H), 2.52-2.44 (m, 8H), 1.67 (m, 8H), 1.40-1.28 (m, 44H) 0.89 (t, J = 7.2 Hz, 6H).

^{13}C NMR (100MHz, CD$_3$OD+CDCl$_3$): 174.91, 159.74, 144.40, 125.92, 59.31, 49.11, 32.90, 31.78, 29.74, 29.49, 29.38, 29.34, 29.19, 29.08, 27.93, 26.87, 26.31, 25.09, 22.45, 13.23.

Elemental analysis. Calcd. for $C_{52}H_{90}N_4O_8S_2$ 7H$_2$O: C, 57.32; H, 9.62; N, 5.14. Found: C, 58.73; H, 9.45; N, 4.88.
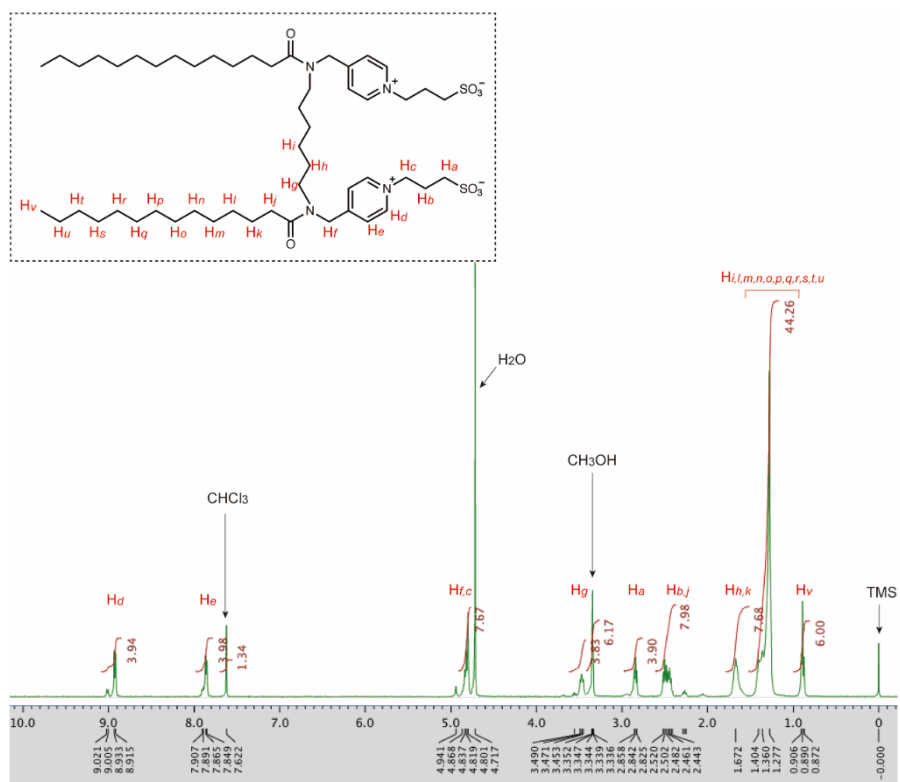
Figure S16. ^{1}H NMR spectrum of **GZI**.

16. Self-organization behavior of GZI and the GZI/HTf₂N mixtures
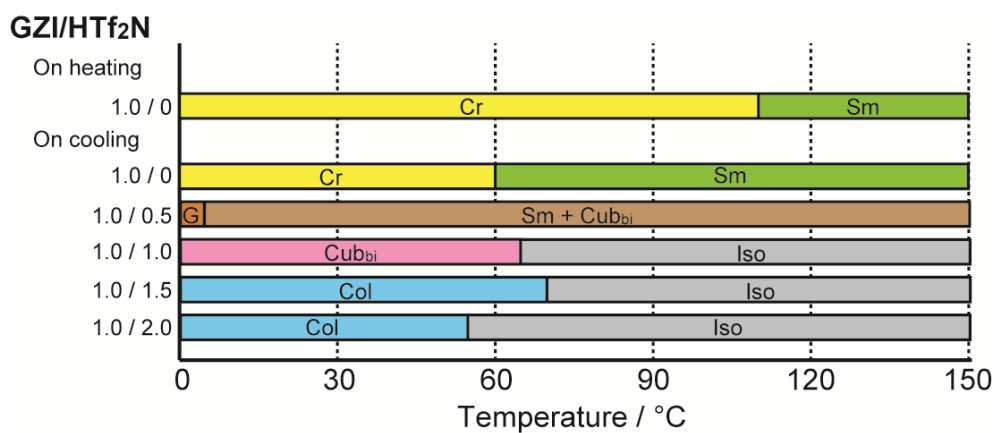
Figure S17. Thermotropic liquid-crystalline behavior of the mixtures of **GZI** and HTf$_2$N in various molar ratios. Cr; crystalline, Sm; smectic, G; glassy, Cub$_{bi}$; bicontinuous cubic, Iso; isotropic liquid, Col; columnar.
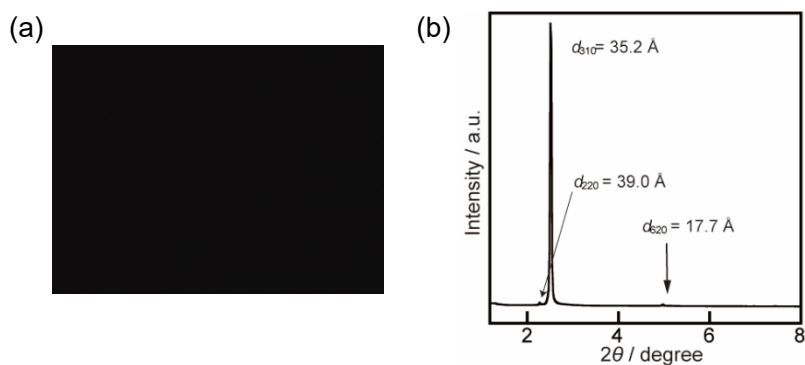
Figure S18. (a) POM image of **GZI**/HTf$_2$N (1.0/1.0 by mol) at 30 °C in the Cub$_{bi}$ phase. (b) XRD pattern of **GZI**/HTf$_2$N (1.0/1.0 by mol) at 30 °C in the Cub$_{bi}$ phase.
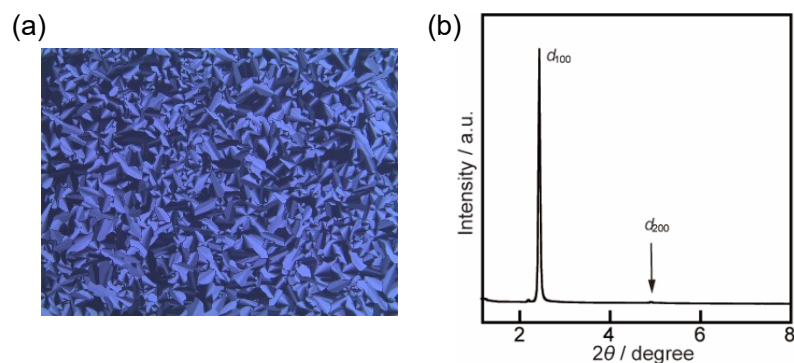
Figure S19. (a) POM image of **GZI**/HTf$_2$N (1.0/2.0 by mol) at 30 °C in the columnar phase. (b) XRD pattern of **GZI**/HTf$_2$N (1.0/2.0 by mol) at 30 °C in the columnar phase.
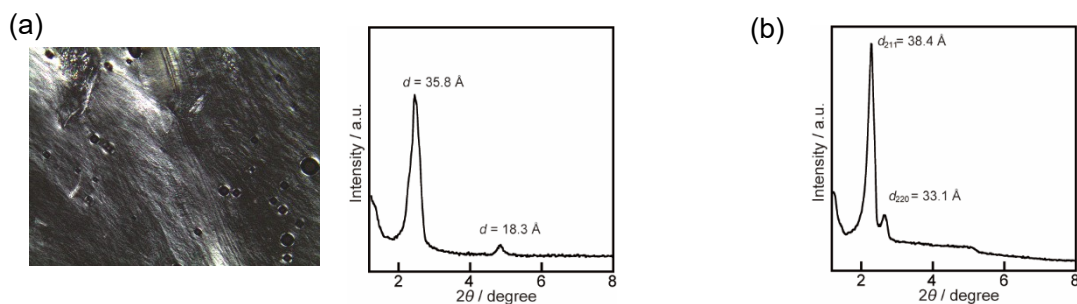
Figure S20. (a) POM image and XRD pattern of **GZI**/HTf$_2$N (1.0/0.5 by mol) containing 15.6 wt% H$_2$O at 30 °C. (b) XRD pattern of **GZI**/HTf$_2$N (1.0/0.5 by mol) containing 20.0 wt% H$_2$O at 30 °C in the Cub$_{bi}$ phase. Taking into account these LC behavior of **GZI**/HTf$_2$N (1.0/0.5 by mol) with various water contents, it is assumed that **GZI**/HTf$_2$N (1.0/0.5 by mol) containing 15.6 wt% H$_2$O (a non-polymerizable control sample) forms a LC phase in which smectic and Cub$_{bi}$ phase domains are co-existing.

Reference

1. Y. Jung, K. T. Chu, S. Torquato, *Journal of Computational Physics,* 2007, **223**, 711.